Electrical Detection of Nucleic Acid Amplification Using an On-Chip Quasi Reference Electrode and a PVC REFET

Eric Salm[ab], Yu Zhong[bc], Bobby Reddy Jr. [bc], Carlos Duarte[bc], Vikhram Swaminathan[bd], Yi-Shao Liu[e] and Rashid Bashir[abc]

[a] Department of Bioengineering, University of Illinois at Urbana-Champaign, Urbana, 61801, IL, USA.
[b] Micro and Nanotechnology Laboratory, Urbana, 61801, IL, USA
[c] Department of Electrical and Computer Engineering, University of Illinois at Urbana-Champaign, Urbana, 61801, IL, USA.
[d] Department of Mechanical Science and Engineering, University of Illinois at Urbana-Champaign, Urbana, 61801, IL, USA
[e] Taiwan Semiconductor Manufacturing Company, Hsinchu, Taiwan

Abstract

This supplementary section serves to expand upon concepts presented in the main article. The initial section highlights the method for determining the pH change associated with nucleic acid amplification. The calculations focus on the effects of buffer pKa, buffer concentration, starting pH, and DNA yield. The supplementary figures presented include calibration measurements, a schematic representation of pH sensing with a quasi-reference electrode, the effect of priming the platinum electrode before performing the experiment, using this method for droplet-in-oil pH measurements, and using a standard reference electrode and an ISFET for detection of nucleic acid amplification. These figures provide necessary supplementary data to extend the reader's understanding as well as present alternative methods for using the ISFET/REFET to detect nucleic acid amplification.

Calculating the Change in pH associated with Nucleic Acid Amplification

This method applies the Henderson-Hasselbalch equation to determine the change in pH associated with a change in hydrogen ions in solution (see equation 1). To start, the buffering components on the solution must be identified, as well as the starting pH. For the Isothermal Amplification Buffer, around pH 7-8, the buffering capacity comes from the 20mM Tris-HCl in solution (pKa 8.08). The starting pH is taken to be pH 8 for these calculations. At this pH, the reaction is below the pKa of Tris-HCl. As the buffering capacity is strongest around the pKa value, it is best to start the reaction below the pKa to ensure the largest potential pH change.

$$pH_o = pK_a + log_{10}(\frac{[A^-]}{[HA]})$$

Equation 1: Henderson-Hasselbalch Equation

First determine the starting A^- and HA concentration for your given Tris-HCl concentration and pH.

At pH_o 8, pK_a 8.08, and 20mM Tris-HCl:
A^- + HA = 20mM
A^- = 9.082mM
HA = 10.918mM

For a 500ug/mL LAMP yield, the generated hydrogen ions $[H^+]$ = 1.515mM. For a 40ug/mL PCR yield, the generated hydrogen ions = 0.121mM.

To determine the change in pH associated with generation of hydrogen ions, we apply the Henderson-Hasselbalch equation a second time. In this calculation, the concentration of A- has been reduced by $[H^+]$. The HA concentration has been increased by $[H^+]$.

$$\Delta pH = pH_o - (pK_a + log_{10}\left(\frac{[A^-] - [H^+]}{[HA] + [H^+]}\right))$$

Equation 1: Delta pH with Henderson-Hasselbalch Equation

The delta pH for LAMP = -0.136.
The delta pH for PCR = -0.01.

For reaction optimization, the Henderson-Hasselbalch equation states that changing the buffer (pK_a), the buffer concentration (A^- +HA), the starting pH (pH_o), or the yield of the reaction (H^+) will affect the overall ΔpH.

Supplementary Figures

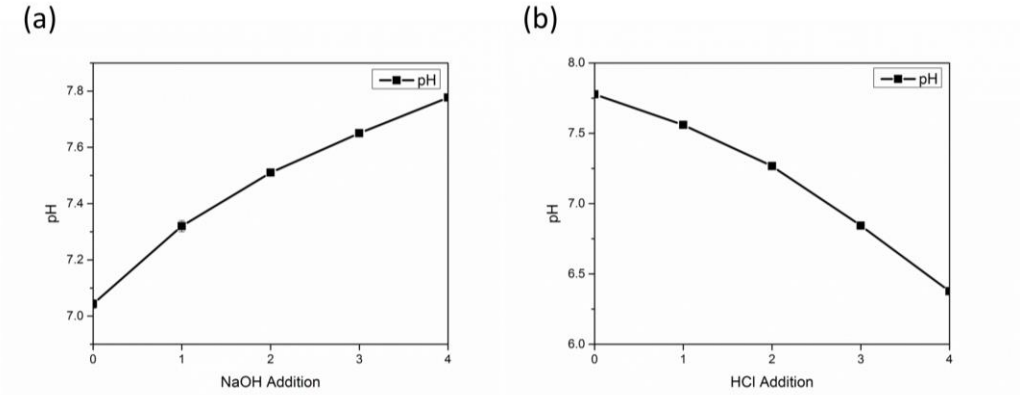

Supplementary Figure S-1. *pH Calibration Curves* The curves shown here depict the changes in pH associated with four NaOH and four HCl additions. Given the pKa of Tris-HCl is 8.08, the curves can be seen to flatten out as they approach pH 8.08.

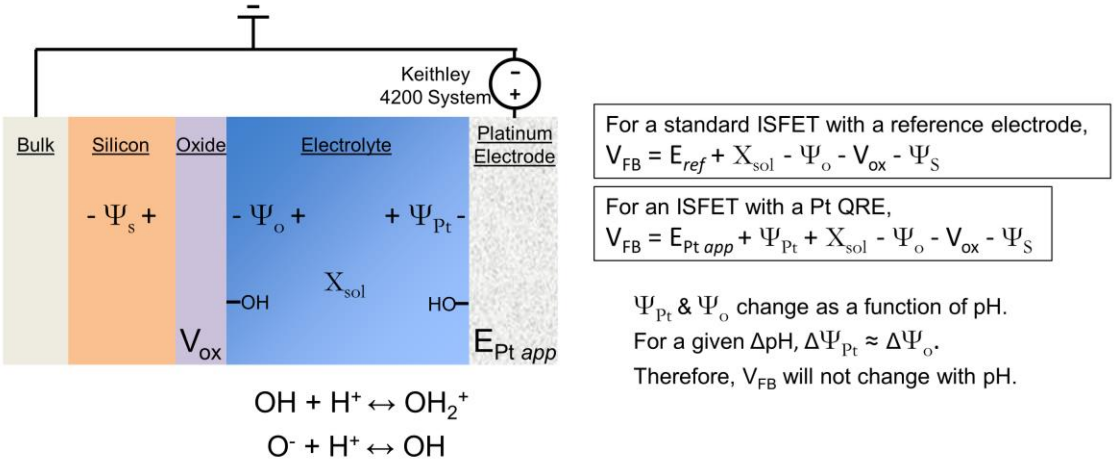

Supplementary Figure S-2. *Basis for Lack of pH Response with QRE* A schematic of an ISFET system is shown. A bias is applied to the electrolyte using a platinum electrode. The surface potential at the platinum electrode and the oxide change as a function of pH. The change at the platinum electrode and the oxide are approximately equal, but have opposite signs. This results in no change in the system's flatband voltage and results in minimal change in the ISFET response. A PVC layer on the ISFET serves to block the pH response of the oxide surface. In doing so, the change in surface potential at the electrode can be measured using the FET. The equations were derived from Bergveld et al. 2003.(13)

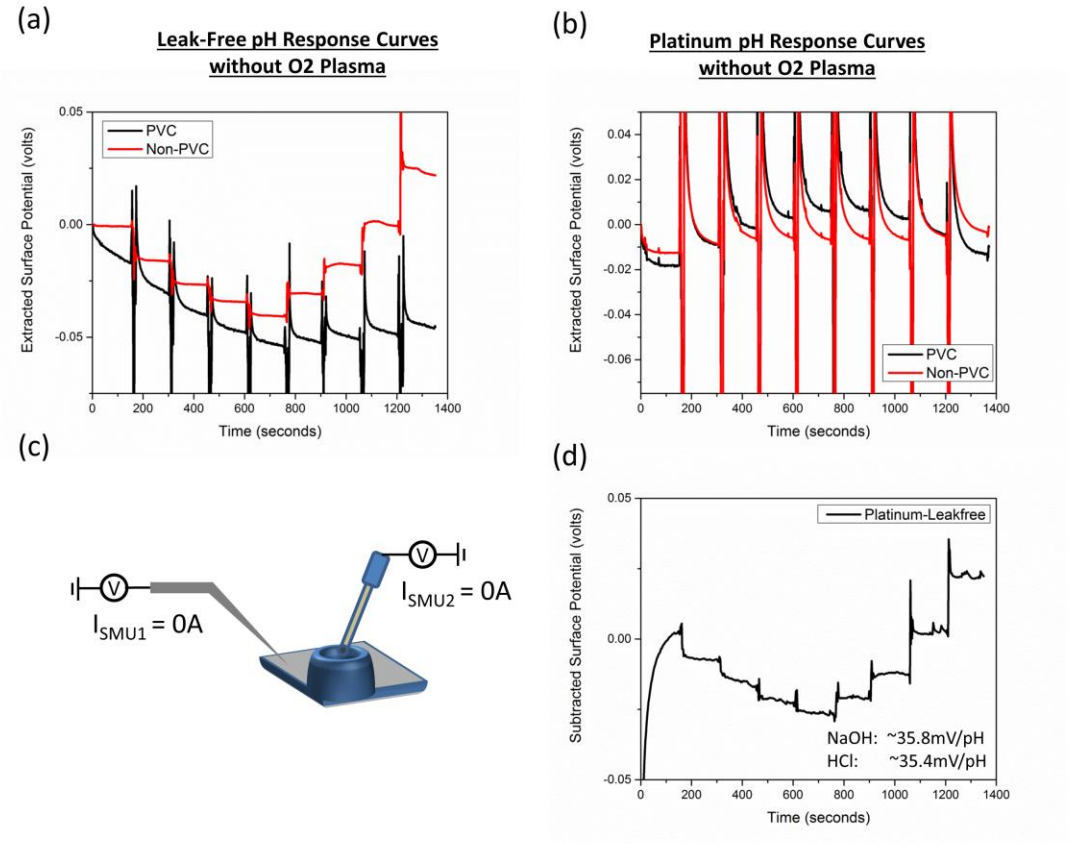

Supplementary Figure S-3. *O2 Plasma Treatment of On-Chip Platinum* (a) Leak-free reference electrode device response curves without an O2 plasma treatment. The ISFET responds well without O2 plasma treatment when swept with the leak-free electrode. (b) When the platinum is not exposed to oxygen plasma before measurements, the pH sensitivity of the platinum is slow and unstable. (c) and (d) The instabilities of the platinum pH response can also be seen in the open circuit potential measurement of the non-O2 plasma-treated platinum vs. the leak-free reference electrode.

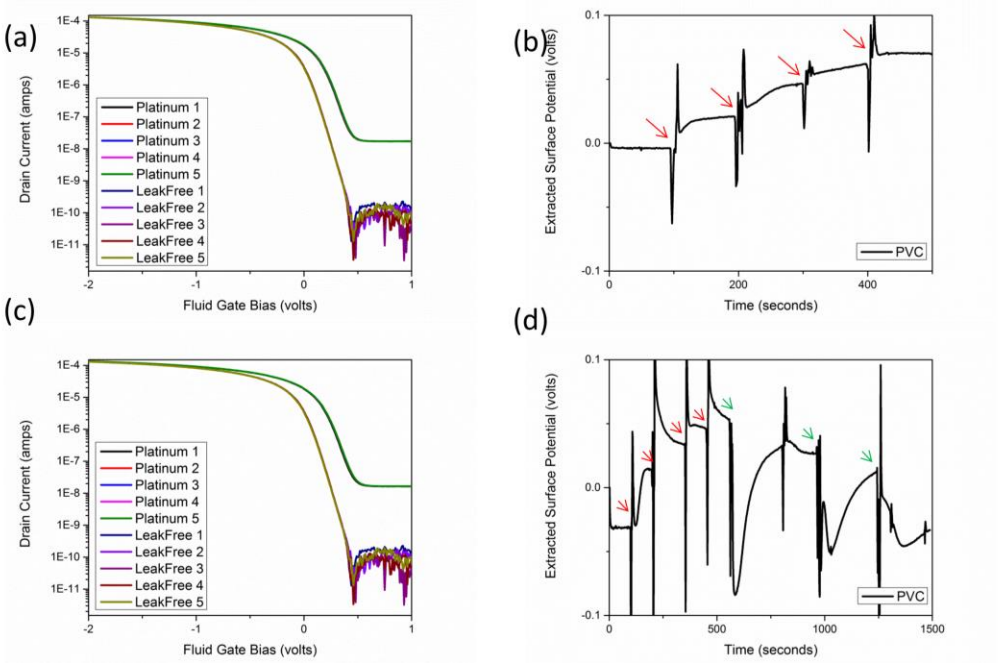

Supplementary Figure S-4. *Droplet-in-Oil pH Response* (a) and (b) Depict HCl and/or NaOH additions into droplets-in-oil. To aid NaOH or HCl injection, the droplets were large at 20uL; however, this test proves that droplet-in-oil pH testing is possible with the PVC-REFET plus platinum electrode configuration.

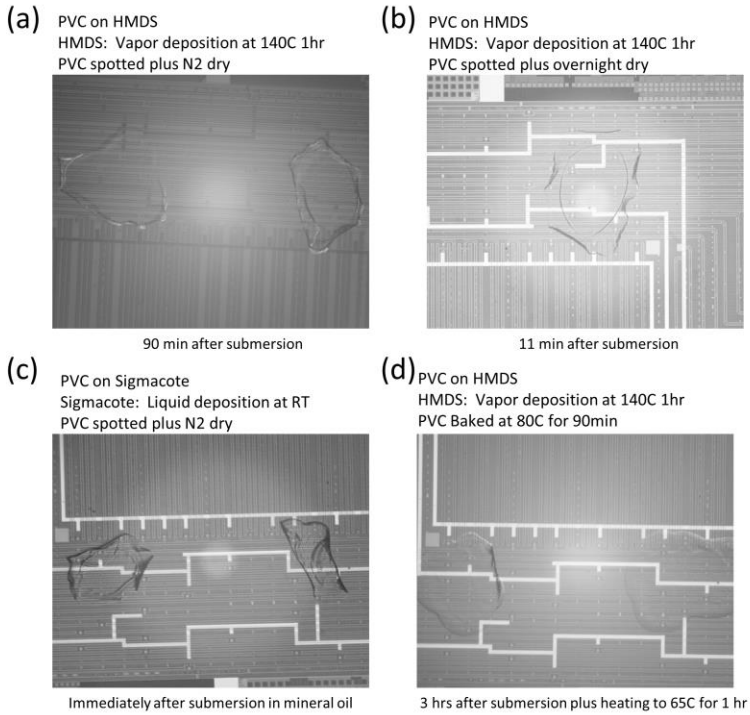

Supplementary Figure S-5. *PVC Stability in Mineral Oil* (a) PVC on HMDS without any thermal curing step results in PVC-liftoff at room temperature in mineral oil. (b) PVC on HMDS without thermal treatment, but with an overnight drying step also resulted in liftoff at room temperature in mineral oil (c) Using sigmacote, a common silane for on-chip PCR passivation, resulted in almost immediate liftoff of the PVC. (d) Baking the PVC at 80C provided a substantial increase in PVC stability even when heated to 65C for 1 hour.

(a)

(b)

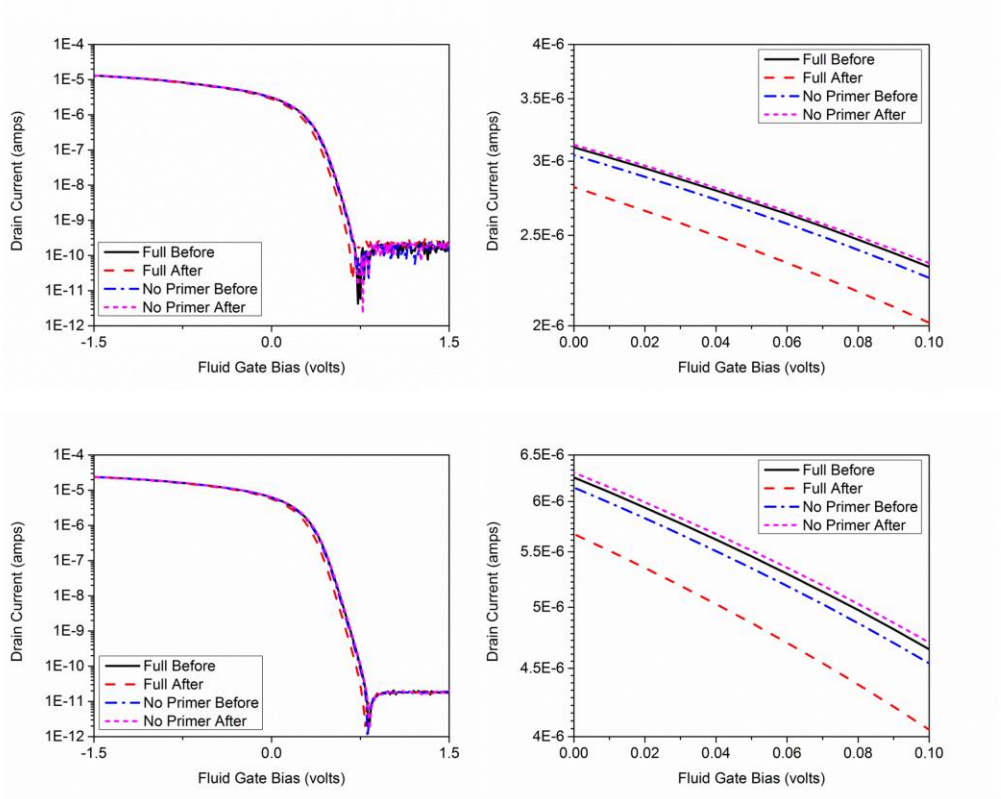

Supplementary Figure S-6. *Endpoint pH-LAMP with a Leak-Free Reference Electrode* (a) and (b) Examples are shown where detection was carried out with a leak-free electrode in solution. As expected, and with the opposite trend to the platinum electrode example, the threshold voltage shifts to a more negative value after amplification. The pH change for full amplification was measured to be ~-0.6 units.

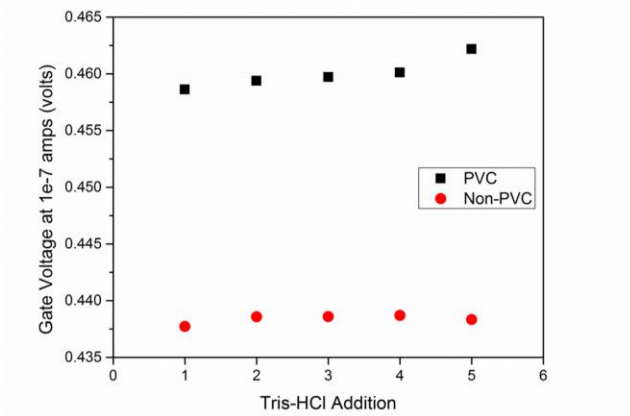

Supplementary Figure S-7. *Threshold Voltage Stability with Solution Exchange* Two devices were measured, a PVC device (LSP61) and a non-PVC device (LSP94) and the solution exchanged 5 times. Between each solution exchange, the device was rinsed via pipetting 3 times. Minimizing variations in threshold voltage is necessary for robust endpoint detection experiments. Issues such as electrostatic discharge within the device can result in large threshold voltages shifts if they are not controlled. The PVC device showed an average change from step 1 of 1.7mV, st. dev. = 1.26mV. The non-PVC device shows an average change of 0.82mV, st. dev. = 0.16mV. The change is considerably less than the 66mV change seen in the Full amplification result from Figure 5(c).